CODEN IEJMAT *Internet Electronic Journal of Molecular Design* **2006**, *5*, 150–167 ISSN 1538–6414
BioChem Press http://www.biochempress.com

Inter*net* Electronic Journal of Molecular Design

March 2006, Volume 5, Number 3, Pages 150–167

Editor: Ovidiu Ivanciuc

Proceedings of the **International Symposium on Carbon Materials – Theoretical and Experimental Aspects**, Budapest, October 24–26, 2005

The C_3 Puzzle: Formation of and Spontaneous Emission from the C_3 Radical in Carbon Plasma

László Nemes,[1] Anna M. Keszler,[1] Christian G. Parigger,[2] James O. Hornkohl,[2] Hope A. Michelsen,[3] and Vadim Stakhursky [4]

[1] Chemical Research Centre of the Hungarian Academy of Sciences, Institute of Structural Chemistry, Laser Spectroscopy Laboratory, Pusztaszeri út 59–67, H–1025 Budapest, Hungary
[2] University of Tennessee, Space Institute, Tullahoma, Tennessee 37388, U.S.A.
[3] Combustion Research Facility, Sandia National Laboratories, Livermore, CA 94550, U.S.A.
[4] Laser Spectroscopy Facility, Department of Chemistry, Ohio State University, Columbus, OH 43210, U.S.A.

Received: December 8, 2005; Revised: February 2, 2006; Accepted: February 6, 2006; Published: March 31, 2006

Citation of the article:
L. Nemes, A. M. Keszler, C. G. Parigger, J. O. Hornkohl, H. A. Michelsen, and V. Stakhursky, The C_3 Puzzle: Formation of and Spontaneous Emission from the C_3 Radical in Carbon Plasma, *Internet Electron. J. Mol. Des.* **2006**, *5*, 150–167, http://www.biochempress.com.

Inter*net* Electronic Journal of Molecular Design

BioChem Press
http://www.biochempress.com

The C_3 Puzzle: Formation of and Spontaneous Emission from the C_3 Radical in Carbon Plasma

László Nemes,[1,*] Anna M. Keszler,[1] Christian G. Parigger,[2] James O. Hornkohl,[2] Hope A. Michelsen,[3] and Vadim Stakhursky [4]

[1] Chemical Research Centre of the Hungarian Academy of Sciences, Institute of Structural Chemistry, Laser Spectroscopy Laboratory, Pusztaszeri út 59–67, H–1025 Budapest, Hungary
[2] University of Tennessee, Space Institute, Tullahoma, Tennessee 37388, U.S.A.
[3] Combustion Research Facility, Sandia National Laboratories, Livermore, CA 94550, U.S.A.
[4] Laser Spectroscopy Facility, Department of Chemistry, Ohio State University, Columbus, OH 43210, U.S.A.

Received: December 8, 2005; Revised: February 2, 2006; Accepted: February 6, 2006; Published: March 31, 2006

Internet Electron. J. Mol. Des. **2006**, *5* (3), 150–167

Abstract

In this review work we address the problem of observing spontaneous emission from the Swings transitions of the C_3 radical in laser–generated graphite plasma. We summarize the spectroscopy of the C_3 radical in carbon vapor and plasma, sketch the chemical routes leading to this carbon cluster under plasma conditions, review some theoretical calculations, and then present our own emission spectroscopy, experimental investigations. We report time–averaged, laser–induced optical breakdown spectra from Nd:YAG laser generated graphite micro–plasma. In 200–300 torr of argon and helium, a weak emission continuum was observed centered at 400 nm when using laser fluence of about 1 J cm^{-2}. We conclude that observation of the 400 nm carbon plasma continuum depends critically on the experimental configuration. Assignment of this continuum to the C_3 radical is not as straightforward as may have been thought previously. Further possibilities are considered for the origin of this continuum.

Keywords. C_2 radical; C_3 radical; laser induced carbon plasma; laser induced incandescence; quenching; quantum chemical calculations; spectral simulation.

Abbreviations and notations

Bremsstrahlung, free-free radiation	LII, laser induced incandescence
LIBS, laser induced breakdown spectroscopy	LIF, laser induced fluorescence
LTE, local thermodynamic equilibrium	PAH, polycyclic aromatic hydrocarbons
FC, factors Franck–Condon factors	YAG, yttrium aluminum garnet
Vibronic, vibrational–electronic	

Presented in part at the International Symposium on Carbon Materials – Theoretical and Experimental Aspects, Budapest, October 24–26, 2005.

* Correspondence author; phone: 36–01–348–1100; fax: 36–01–325–7892; E–mail: nemesl@chemres.hu.

1 INTRODUCTION

The C_3 molecule is one the most studied triatomic molecules in the history of spectroscopy. In a relatively recent survey on carbon cluster spectroscopy, structure and energetics [1], a thorough review of the literature up to 1998 was provided. C_3 was first detected in a comet spectrum in 1881 [2], and its first laboratory spectrum was recorded in 1942 [3], although the spectrum was attributed to the CH_2 radical. The final assignment of the spectral features in the so–called Swings–bands of C_3 in the laboratory was made in 1951 [4], and the first detailed vibrational–electronic (vibronic) analysis of the 4050 Å laboratory spectrum was published in 1963 [5] and in more detail in 1965 [6]. There were a great number of high resolution analyses of the low temperature (mainly molecular beam) spectra of C_3 in the optical and infrared ranges between 1965 and 1998, and the van Orden–Saykally review [1] contains numerous references from this period.

In this work we are concerned with the spectral continuum around 4000 Å (400 nm) observed in high temperature sources, such as equilibrium carbon vapors, flames and carbon plasmas investigated by various emission and absorption spectroscopic methods. Assuming that this continuum arises from a great number of individual transition lines, it is commonly referred to as a 'pseudo–continuum' or 'line continuum' emphasizing that it arises from bound–bound transitions and not from free–free or free–bound true continuum transitions. Many observations of such continua have also been made previously, we refer here to a representative subset without claiming a full coverage of such studies [7–26]. The continua observed in carbon vapors and plasmas are attributed to several possible sources, mostly but not exclusively to radiation from the C_3 radical, as will be discussed later.

2 THE CREATION OF C_2 AND C_3 IN CARBON VAPOR AND PLASMA

The creation of the C_2 and C_3 radicals and other smaller carbon linear clusters in carbon vapors and plasmas is a subject that has been described in a great number of papers, usually in discussions on the growth of large carbon clusters. In this work we limit our attention to the formation of the C_2 and C_3 radicals. Again, without the claim of complete coverage a few works are mentioned (Refs. [27–41]). Some theoretical calculations in this respect will be reviewed in the next section. The thermodynamic properties of carbon have been studied extensively. Reference [29] provides a good review of this work. Vapor pressure measurements above solid and liquid carbon showed that above 2000 K C_3 is the dominant species in equilibrium carbon vapor with C_2 next to it in abundance. Larger members of the linear chain carbon molecules occur at lower abundances.

Both the C_2 and C_3 radicals may be formed by bimolecular or termolecular addition reactions, by direct ablation from target surfaces and from the mantles of macroscopic carbon particles. The

direct production of C_2 and C_3 molecules by detachment from graphitic sheets was approached early on using a simple statistical mechanical picture valid for equilibrium carbon vapors [42]. This work hypothesized that C_2 and C_3 dissociate from the edge of graphene sheets and was aimed at the determination of the heat of sublimation of graphite. Although the value for the heat of sublimation given in Ref. [42] is now superseded by newer and better estimates, the classical arguments for C_2 and C_3 production from the graphene sheets are still valid.

The possible molecular formation of the carbon clusters in carbon vapors and plasmas may be described by the following routes [31]:

$$C_x + C_y + M \rightarrow C_{x+n} + C_{y-n} + M \quad (1)$$

$$C_x + C_y \rightarrow C_{x+n} + C_{y-n} \quad (2)$$

$$C_x + C_y \rightarrow C_{x+y} \quad (3)$$

When $x = y = n = 1$, routes (2) and (3) are identical, and (1) is only different as it indicates a termolecular reaction involving a buffer atom that usually is a rare gas atom (He or Ar). Thus C_2 may be created by two triplet ground state carbon atoms $C(^3P)$, and the C_2 molecule could arise either in the direct reaction (2) or (3) in the triplet state $a^3\Pi_u$ or in the termolecular reaction (1) that may result in the true ground state $X^1\Sigma^+_g$ (as opposed to the usually greatly populated metastable $a^3\Pi_u$ state). The presence of a third body lifts the Wigner–Witmer diatomic molecule formation spin correlation rule [43] that was later extended to the formation of linear triatomic molecules by Herzberg [44] (see also Ref. [45]) and allows the formation of a singlet product from two triplet components.

Experimental estimates for the heats of formation and the total atomization (dissociation energy) for C_2 are found in a number of papers (*e.g.* in [1]), Ref. [1] gives ΔH^o_f =195(2) and ΣD_o = 144(2) kcal/mol.

Spectroscopic observations of C_2 in carbon plasmas can provide information about its formation under such conditions. The most frequently observed vibronic transition of C_2 between 430 and 700 nm are the Swan transitions for which the upper state is the $d^3\Pi_g$ level. This state has a free radiative lifetime around 100 ns, depending on vibrational excitation [35]. The Swan transitions, found by time resolved emission spectroscopy of carbon plasmas, are observable for more than 100 microseconds [41]. These observations imply a long term mechanism that repopulates the $d^3\Pi_g$ level of the C_2 radicals, or freshly creates excited C_2 radicals over this longer period. Monchicourt [19] argues on the basis of temporal and spatial distributions of electronically excited carbon clusters, C_2 and C_3, that excited C_2 radicals are formed according to Eq. (3) when rapidly expanding neutral carbon atoms collide with slower neutral carbon atoms in the plasma, whereas he excludes the possibility of formation by ejection from larger fragments. In these studies focused Nd:YAG laser radiation at 532 nm was at a high laser irradiance of approximately 2×10^8 W cm^{-2} per pulse.

The formation of C_3 radicals could also be assumed to take place either by the molecular mechanisms in Eqs. (1)–(3), or from larger carbon fragments of graphene sheets. There are in principle several vibronic bands of C_3 that could be observed, the so–called Swings bands centered at 405 nm, $A^1\Pi_u - X^1\Sigma^+_g$ (*e.g.*, [5]), the vacuum ultraviolet transitions $^1\Sigma^+_u - X^1\Sigma^+_g$ observed between 160 and 170 nm in matrix isolation spectra [46], and the phosphorescence transition $^3\Pi_u - X^1\Sigma^+_g$ observed also in matrix isolation around 590 nm [47]. No report on this phosphorescence transition has been published to date in the gaseous or plasma state; thus this transition is not likely to occur in carbon plasma emission spectra with easily observable intensity. Therefore detection of C_3 in carbon plasma emission spectra is practically limited to the observation of the Swings bands around 405 nm.

Monchicourt [19] designated the reaction in Eq. (3) as the most probable channel to produce excited C_3 in plasmas. He also concluded from cluster velocity data that the carbon atom in the addition reaction should be in the $C(^3P)$ ground state to produce a stable excited C_3 radical that arises from binary associative collisions between hot C atoms with slow C_2 radicals. He also excluded the possibility for C_3 formation from the graphitic surfaces. Later studies by Krajnovich on KrF laser excited carbon plasmas [38] in the low laser irradiance regime ($2–5\times10^7$ W cm^{-2}) led to the conclusion that, when plasma effects are minimized, the sputtered flux is limited to C, C_2 and C_3 species. However, according to Krajnovich, C_2 and C_3 are emitted directly from the graphite surface and constitute a larger fraction of carbon in the plasma than carbon atoms. This author concluded that thermal heating and laser heating are fundamentally different with respect to material removal mechanisms from the graphite surface. Although laser sputtering appears to be a non–thermal process, cluster size distributions are very similar to those from thermal effects. The reason for this is found in the removal of C_2 and C_3 molecules from graphitic sheet edges, as suggested by Herzberg *et al*. [42]. Because larger cluster splitting from the graphene sheets is disfavored by entropy considerations, the cluster distribution will still be dominated by C, C_2 and C_3.

Experimental photodissociation studies on linear carbon clusters [48] showed that C_3 arises favorably through a low energy dissociation channel $C_n \rightarrow C_3 + C_{n-3}$. This channel is reached by a single–photon mechanism in the UV that involves rapid internal conversion to the ground state of the larger molecule, followed by dissociation. The photofragmentation of carbon cluster cations containing more than 5 atoms also leads to preferential loss of a neutral C_3 fragment [49]. This happens when using low intensities of 248 nm radiation for photodissociation. Thus in carbon plasmas that may contain an ionized fraction of carbon clusters along with higher linear carbon chain analogs, photodissociation may also be a source of neutral C_3 radicals.

There have been theoretical studies on the possible photodissociation channels in linear carbon clusters [50] that support the experimental finding that the energetically most favorable

fragmentation channel for linear carbon clusters C_n (n = 4 to 6) corresponds to the loss of neutral C_3 resulting in C_{n-3} clusters. Moreover, triplet state C_3 may isomerize into a ring shaped equilateral triangular isomer that is the most stable triplet state form for this cluster [51]. There are theoretical calculations underway that suggest that the bimolecular condensation reaction in Eqs. (2) and (3) proceeds smoothly to form singlet C_3 from the triplet ground state carbon atom and the singlet ground state C_2 radical [52]. A linear pathway with no barriers on the S_1 surface was found, which indicates a rapid reaction between C and C_2 in linear collisions. Further calculations will be carried out to study the formation of triplet state C_3.

3 LASER–INDUCED BREAKDOWN EMISSION SPECTROSCOPY IN LASER ABLATION OF GRAPHITE

We have utilized during the past few years time averaged laser–induced breakdown (LIB) plasma emission spectroscopy [53–58] using Q–switched nanosecond Nd:YAG laser radiation, graphite targets and carbon containing gases (C_3H_4·, allene, C_6H_6 benzene and CO_2, carbon dioxide). In our LIB spectra we have so far not detected any significant emission features that could be attributed to the C_3 Swings emission. Thus we were interested in investigating the possibility that this absence might be due to the difficulty in observing the Swings bands under plasma conditions, where the temperature is sufficiently high to wash out any signatures, therefore merging the complex vibronic structure of the Swings bands into the spectral background. In time–averaged breakdown emission spectra there is frequently a broad blue–UV continuum that arises from the bremsstrahlung radiation of hot electrons in the early period of the plasma [59], and this continuum extends to the region of the Swings bands around 405 nm.

3.1 Simulation of the Vibronic Structure of the C_3 Swings Bands

To check the expected high temperature band contour of the Swings bands, we have started the exact computer simulation of the C_3 Swings transitions. The software (SpecView) for doing such simulations was written by Dr. Vadim Stakhursky at the Ohio State University [60]; all inquiries concerning the SpecView simulaton code details should be addressed to him. In order to carry out such simulations, detailed spectroscopic constants are needed. The various vibronic constants for the transitions building up the Swings bands were compiled from the literature on low temperature, high resolution, gas–phase spectroscopic measurements, carried out mostly in molecular beams [62–68], and theoretical Franck–Condon (FC) factors were taken from the work of Jungen and Merer [61]. A detailed report on these simulations is in progress. We have presently used a maximum of 44 vibronic bands, and the spectroscopic constants in the Swings transitions were selected from Refs. [6,61,65,66]. The simulations were performed up to rotational quantum number J = 400 and used a Doppler broadening value (0.3 cm^{-1}) corresponding to temperatures T = 3000,

5000 and 7000 K for C_3.

The simulation in Figure 1 is only an approximate one for several reasons. First only the bending (ν_2) progressions are taken into account, and the maximum vibrational excitation is only v = 8. Second, only thermal Doppler broadening was taken into account since nothing is known about the plasma broadening of the rotational lines in the Swings transitions. Finally centrifugal distortion at high J values is probably significant, but because there are no experimental data for it, we used only a rigid rotor approximation. The structured high frequency side of the simulated band as compared to the smooth high temperature experimental contours in hot carbon vapors (*e.g.* [12]) is most probably due to the neglect of many vibronic components, *i.e.*, those with high vibrational quantum numbers for the bending mode, and progressions of the excitation of the symmetric (ν_1) and antisymmetric (ν_3) stretching modes of C_3. To take these missing vibronic components into account in the simulation, one would need detailed spectroscopic parameters for high bending and stretching excitations, and these are not yet available. In particular nothing is known about the values of the FC factors for the asymmetric stretch progressions, as opposed to the available accurate theoretical values for the bending progressions [61]. Since the mode frequency of the antisymmetric stretch is reduced significantly with the Swings excitation (see, *e.g.*, [66]), such progressions are expected to contribute to the complicated band profile. So far there are no theoretical estimates available for the asymmetric stretching and mixed stretching–bending FC factors for the Swings bands of C_3.

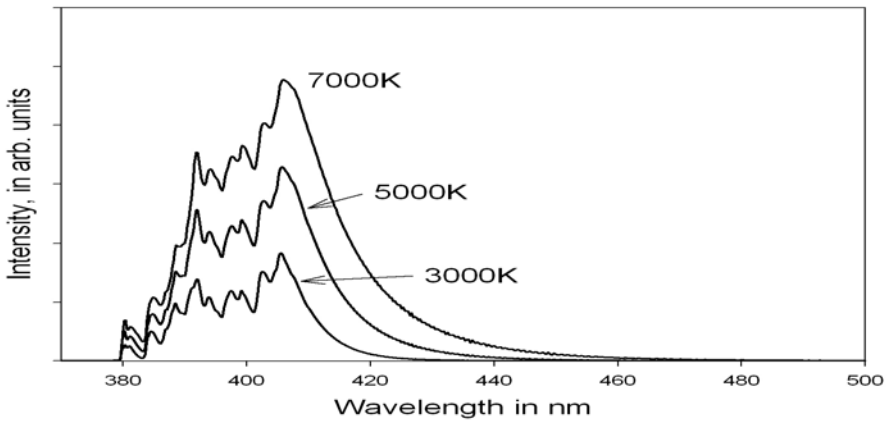

Figure 1. Simulation of the structure of the C_3 Swings transitions at T = 3000, 5000 and 7000 K.

Nonetheless the approximate simulation in Figure 1 shows that even at very high temperatures the Swings bands would have a recognizable profile, not merging completely into the spectral background.

3.2 Spectral measurements of graphite LIB spectra

To complement our previous experiments in which the Nd:YAG laser radiation was focused onto the graphite target or focused into a carbon containing gas [54–57], we carried out analogous

experiments with unfocused laser radiation. These experiments were planned to reduce laser fluence, and were based on the assumption that less intense laser irradiation will allow enough ground state carbon atoms C(^{3}P) and ground state ($X^1\Sigma^+_g$) or metastable $a^3\Pi_u$ C_2 radicals to form the C_3 radicals via Reactions (1–3). The C_3 radicals would then radiate from the excited state $A^1\Pi_u$ to form the Swings emission. Also at reduced laser fluence multiphoton dissociation of the C_3 radicals is expected to be less efficient than at fluences produced by focused laser beams.

The 10 Hz Nd:YAG laser was used at the fundamental wavelength 1064 nm with reduced pulse energies (maximum pulse energy is around 350 mJ). In order to lower the intensity we have used a smaller than optimal delay between the flash lamp trigger and the Q–switch trigger, in the range of 115 and 160 microsecond (optimal delay is around 190 microsecond). The laser beam diameter is 5 mm, and the pulse length is nominally 3.9 ns. Thus at optimum delay we have about 1.8 J cm^{-2} fluence and about 460 MW cm^{-2} irradiance on the target with the unfocused laser in contrast to the focused case, where, assuming a focal spot diameter of 0.2 mm, the fluence is around 1100 J cm^{-2} , and the irradiance is increased to 280 GW cm^{-2}, *i.e.*, by ~ 3 orders of magnitude.

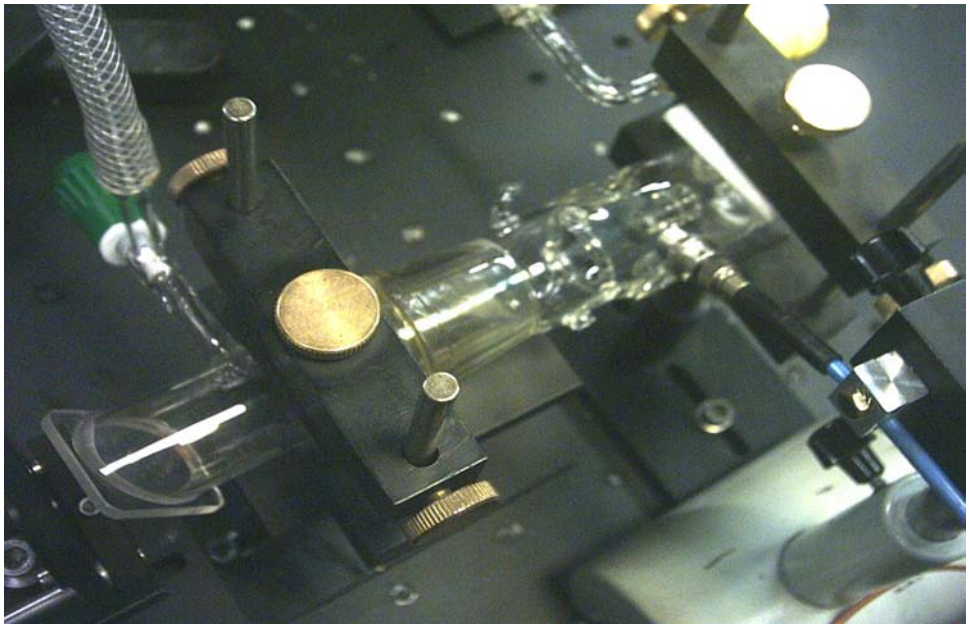

Figure 2. The optical arrangement for the LIBS experiments (laser not shown).

The LIBS cuvette arrangement is shown in Figure 2. Spectra were taken with a fiber optic mini spectrometer WaveStar U (Ophir Optronics) with the longest exposure of 7.353 seconds. Thus about 73 spectra were averaged. The photo in Figure 2 shows the evacuable glass cell and the fiber optic arrangement. In the cell a spectrally pure, stationary graphite disc was placed as the laser target. The laser induced plasma is seen in Figure 3 as a frame from a video recording taken with a digital photo camera.

Figure 3. Photograph of the laser induced carbon plasma in helium background gas.

4 EXPERIMENTAL RESULTS

Figure 4 shows a typical graphite LIB spectrum, as obtained in vacuum with focused 1064 nm radiation. The laser fluence was about 290 J cm^{-2} and irradiance about 48 GW cm^{-2} (in this estimate pulse duration was taken to be 6 ns instead of 4 ns, as decreasing the flash lamp trigger – Q switch trigger delay not only decreases the pulse energy but also broadens the laser pulse).

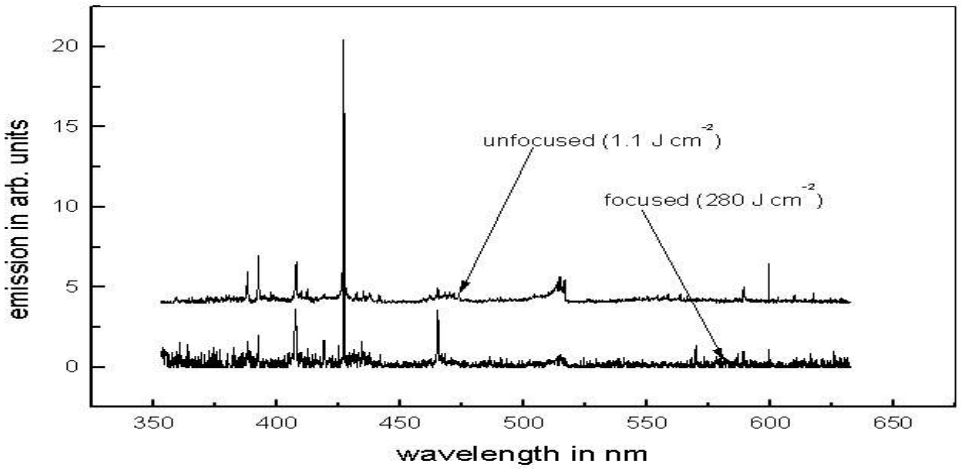

Figure 4. Graphite LIB spectra in vacuum with focused and unfocused 1064 nm laser radiation.

Figure 4 also shows a plasma spectrum obtained in vacuum with unfocused radiation, with a fluence of 1.6 J cm^{-2}. Similar emission spectra in helium and argon background gases were also obtained. Figure 5 shows spectra in Ar, using 1064 nm radiation with a fluence of 280 J cm^2 for the focused beam with an Ar pressure of 5 torr, and fluence of 1.1 J cm^{-2} for the unfocused beam with an Ar pressure of 200 torr. Figure 6 shows a magnified portion of Figure 5.

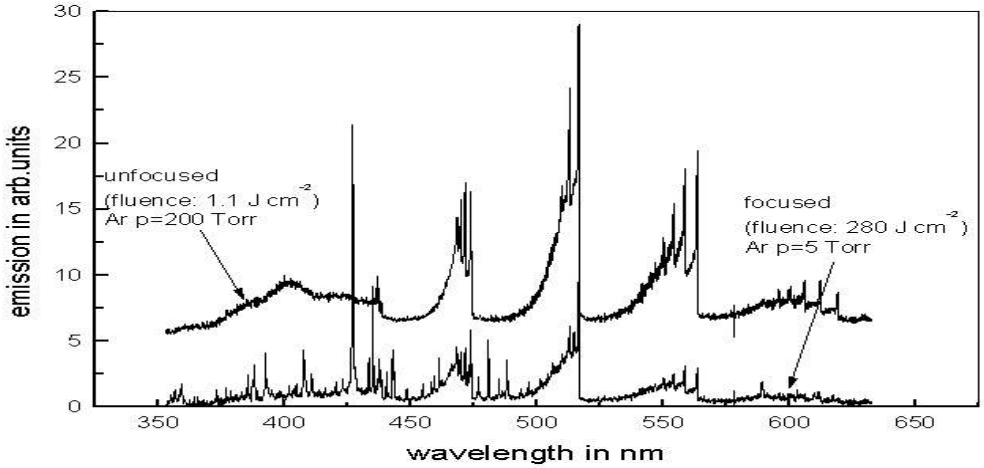

Figure 5. Graphite LIB spectra in argon with focused and unfocused 1064 nm laser radiation.

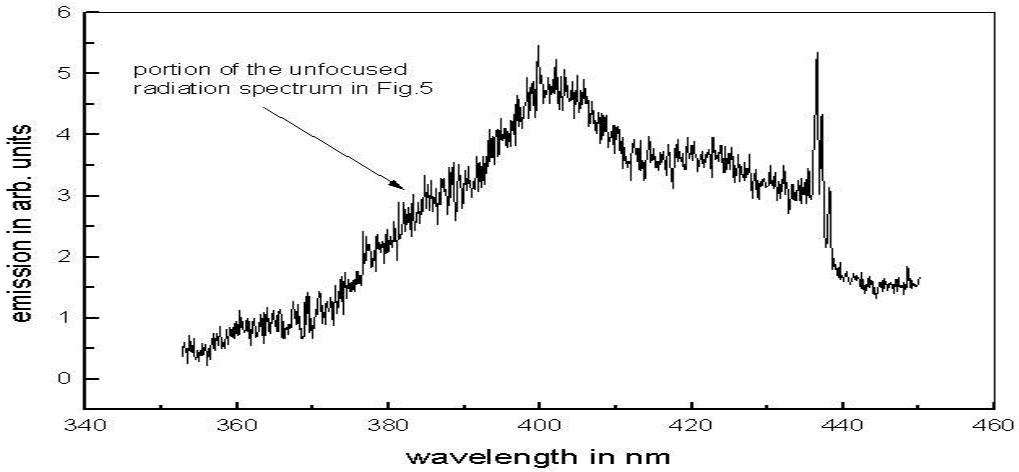

Figure 6. The short wavelength part of the LIB spectrum obtained with unfocused radiation in Figure 5.

A spectrum in helium is shown in Figure 7. It was obtained with an unfocused laser in 300 torr helium at fluence level of 1.1 J cm^{-2}. Spectra taken in helium are weaker hence noisier than those taken in argon. Also the 400 nm continuum is weaker in helium.

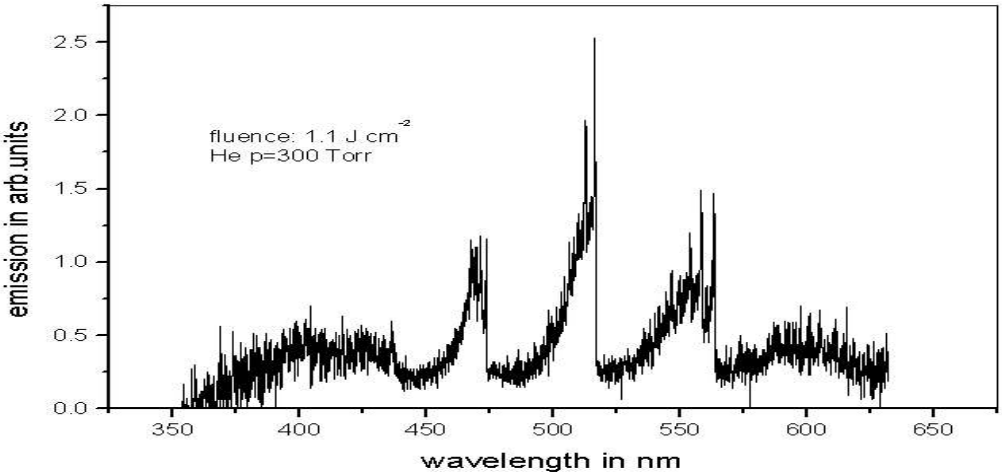

Figure 7. Graphite LIB spectra in helium with unfocused 1064 nm laser radiation at 1.1 J cm^{-2} fluence.

4.1 Analysis of the Emission Spectra

In the emission spectra shown in Figures 4–7 characteristic spectral lines and bands are found, as well as a continuum in some of them. The central issue in this paper is the continuum around 400 nm seen in unfocused experiments using argon and helium background gases. However it is important to note that atomic lines are mainly found in focused experiments (see Figures 4 and 5). The Swan bands of the C_2 radical, on the other hand, are accentuated in the presence of argon and helium but are weak in spectra obtained in vacuum.

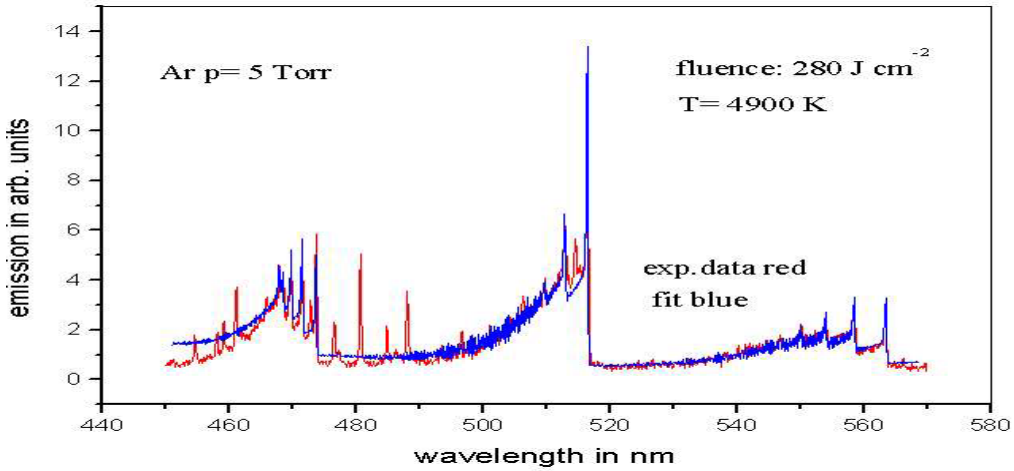

Figure 8. Thermal equilibrium spectral fit to the C_2 Swan bands in argon background gas at focused conditions.

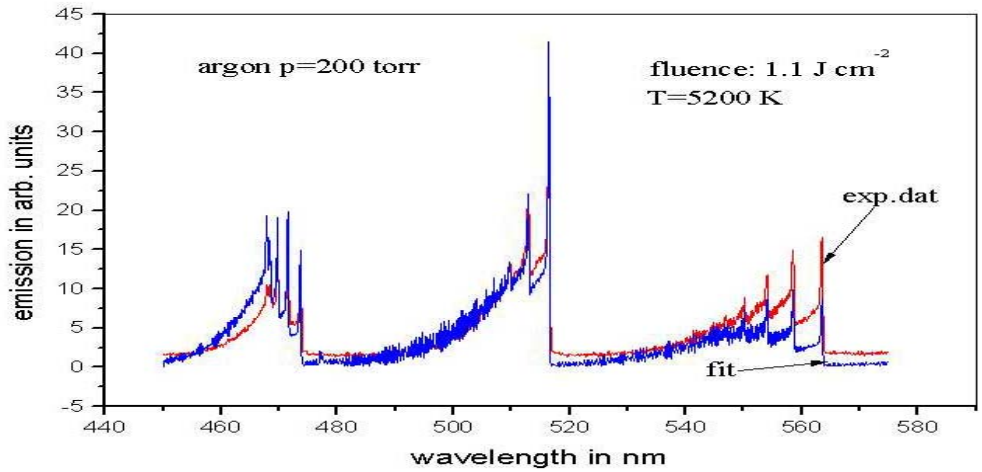

Figure 9. Thermal equilibrium spectral fit to the C_2 Swan bands in argon background gas at unfocused conditions.

Atomic lines appear in the spectra obtained with the focused beam (see Figures 4 and 5). In the low pressure (5 torr Ar) environment only singly ionized carbon lines are found, *e.g.*, at 425 nm (Figure 4), whereas in 200 torr Ar lines belonging to Ar II, ionized carbon are also found, e.g. at 434.9 nm. In vacuum at higher fluences carbon atomic lines also appear in spectra obtained with the unfocused beam (Figure 4).

In Figures 8, 9 and 11 the spectral resolution is high enough to see the vibrational structure of the

$\Delta v = +1$, $\Delta v = 0$ and $\Delta v = -1$ sub–bands of the Swan system at 474, 517 and 564 nm, and some details of the $\Delta v = +2$ and $\Delta v = -2$ sub–bands at 438 and 619 nm in the upper trace in Figure 5. Even the rotational structure is discernible in Figures 8, 9 and 11. Full details on the Swan band structure can be found in many references, *e.g.*, in [77].

Spectral fittings to the vibronic features of the C_2 Swan bands were carried out, using the principles of the exact procedure described in [58,69,70] in order to estimate the vibration–rotation temperature of the C_2 radical in the plasma. The software used for such calculations is a computer program (NMT = Nelder–Mead Temperature) for finding the temperature at which a computed diatomic emission spectrum best fits (in the least–squares sense) an experimental diatomic emission spectrum. Interested readers should contact James O. Hornkohl (jhornkoh@utsi.edu) for a copy of the code.

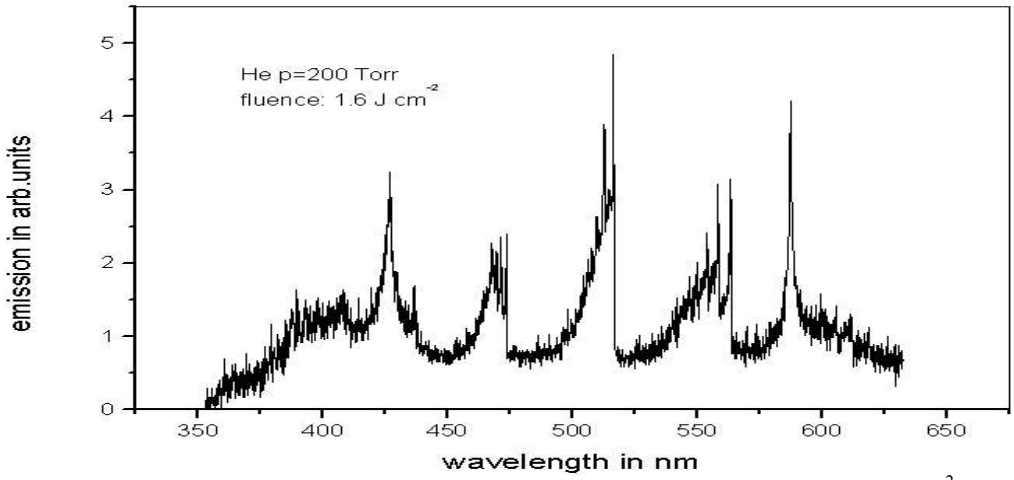

Figure 10. Graphite LIB spectrum in 200 torr helium in unfocused conditions at 1.6 J cm^{-2} fluence.

The quality of the thermal fit is different for the focused and unfocused conditions. When laser radiation is focused, the fit is better, showing that LTE conditions are approached, whereas in unfocused experiments, at low laser fluence no close fit could be achieved for the different vibrational sub–bands of the Swan spectrum, indicating that the assumption of local thermal equilibrium is not valid. Figure 8 shows a fit to the focused experiment in 5 torr Ar and a fluence of 280 J cm^{-2}, and Figure 9 depicts the fit for the unfocused case using 200 torr argon and a fluence of 1.1 J cm^{-2}. However, when laser fluence is increased, atomic lines may appear even in the unfocused case. Under such conditions a broad C II line (singly ionized carbon) appears at 427 nm as shown in Figure 10. From the width of this C II line the value for the electron number density could be derived; however for this purpose one would need several carbon lines in different ionization states [56,57] to derive a value for the electron temperature. Since under unfocused conditions not enough carbon lines are seen in our spectral range, no electron temperature value is obtainable, thus we could not estimate the electron number density. However it must be high enough to lead to near LTE conditions as a fit to Swan bands in Figure 10 is sufficiently good as

can be seen in Figure 11.

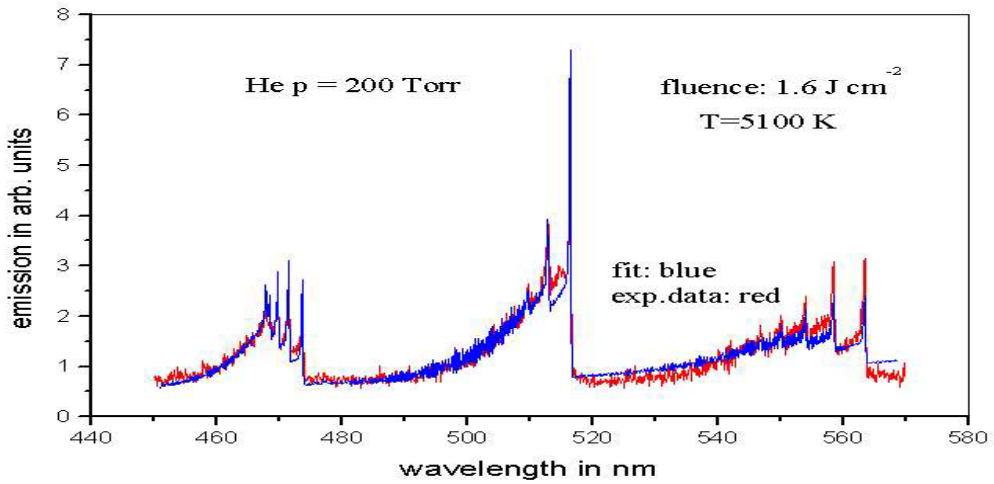

Figure 11. Thermal equilibrium spectral fit to the C_2 Swan bands in helium background gas at conditions for Figure 10.

The thermal fits to the spectra in Figures 8, 9 and 11 gave vibration–rotation temperature values of 4900, 5200 and 5100 K. These temperature estimates are probably correct to ± 200 K for the close fit cases in Figures 8 and 11, but for the non–LTE case in Figure 9 it is difficult to estimate the error.

In our spectra the 400 nm continuum is seen only in emission spectra obtained with the unfocused laser, such as in 200 torr Ar at a fluence of 1.1 J cm^{-2} (Figure 5 and 6) and in helium at pressures 200 and 300 torr and fluences 1.1 and 1.6 J cm^{-2}, respectively (Figures 7 and 10).

5 DISCUSSION AND CONCLUSIONS

The 400 nm continuum was observed in our emission spectra only when unfocused laser radiation was used. This is significant for comparison of our previous studies [54–57] where focused laser beams were used throughout. The continuum is weaker in helium than in argon, although spectra in these rare gas background gases are not strictly comparable because of the weaker intensity in helium. The form of the continuum in our experiments (see Figure 6 of this work) is very similar to spectra reported in the literature earlier [23,24]. Thus we may assume that the continuum we see originates from the same source as in earlier experiments.

However the interpretation of this continuum and similar continua is markedly different from the time resolved, supersonic jet expansion studies in Refs. [18] and [19]. In Ref. [18] continua observed in the range from 300 to 800 nm are attributed to incandescent carbon particle blackbody radiation (as modified by an appropriate spectral emissivity function), whereas in [19] the 400 nm feature is assigned to C_3 Swings emission. In Ref. [18], however, the emission at 400 nm is much broader and does not demonstrate a peak near 400 nm. As we have observed a luminous belt in our

plasmas (see Figure 3) similar to the one reported in Refs. [23] and [24] (where it was attributed to incandescent carbon particulates) it could be assumed that the continuum is contributed by laser–induced incandescence (LII) radiation from the luminous belt. This is a likely interpretation in view of the expected quenching effect of the background rare gases. Kadota and coworkers in their laser–induced fluorescence (LIF) studies [41,71] showed that the population of the (000) vibrational state of the $A^1\Pi_u$ upper state of the Swings transitions (and thus the radiative lifetime of this level) is strongly reduced by collisions with the rare gas atoms or/and by collisions with carbon particles ejected from the target surface. For relatively high background gas pressure, as in our experimental conditions, such quenching effects should eliminate all spontaneous Swings band emission, provided higher excited vibrational states of the $A^1\Pi_u$ electronic state are also collisionally quenched. Even though the quenching data are only available for helium, it may be assumed that at our background gas pressures argon would also be a good quencher. Thus it appears unlikely that the 400 nm continuum in our spectra is due to the C_3 radical.

Another hypothesis is to attribute the 400–nm continuum to carbon particle LII as in [18]. To test this assumption we have carried out preliminary calculations on the shape of LII spectral profiles. Such preliminary results are shown in Figure 12, which shows the predicted emission from 40–nm diameter particles for various model predictions and cases discussed in Ref. [72]. Cases 1 and 2 correspond to emissivity calculated using a Rayleigh–Debye–Gans approximation (Eq. (27)] in Ref. [72]) with $\xi = 0.83$ (Case 1) and $\xi = 1.39$ (Case 2). Cases 3 and 4 represent calculated emissivity using a Rayleigh approximation (Eq. 26 in Ref. [72]) with an index of refraction $m = 1.57 - 0.56i$ (Case 3) and $m = 2.3 - 0.6i$ (Case 4).

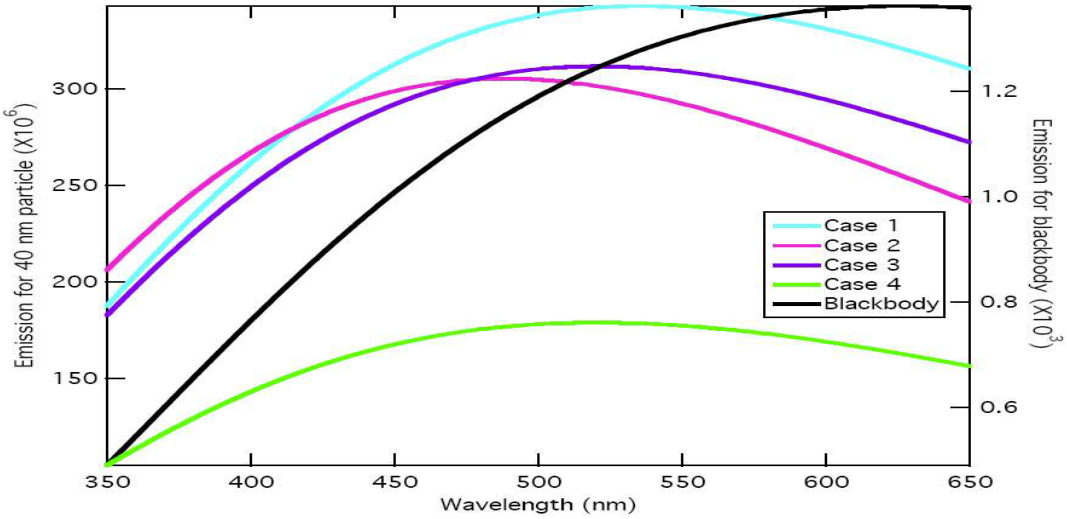

Figure 12. LII spectral curves calculated for various models (cases) in [72].

As seen in Figure 12 a raw blackbody radiation model reaches a maximum near 600 nm, and, when spectral emissivity corrections are used, the maximum is shifted to shorter wavelengths.

A preliminary fit to the spectrum in Figure 5 resulted in a broad continuum when case 2 for carbon particle diameter 100 nm was used; this is shown in Figure 13. Such a fit would be more informative if we could remove from our spectra other contributions to the background, *e.g.*, electron bremsstrahlung. Electron bremsstrahlung, however, is always present in time averaged emission spectra.

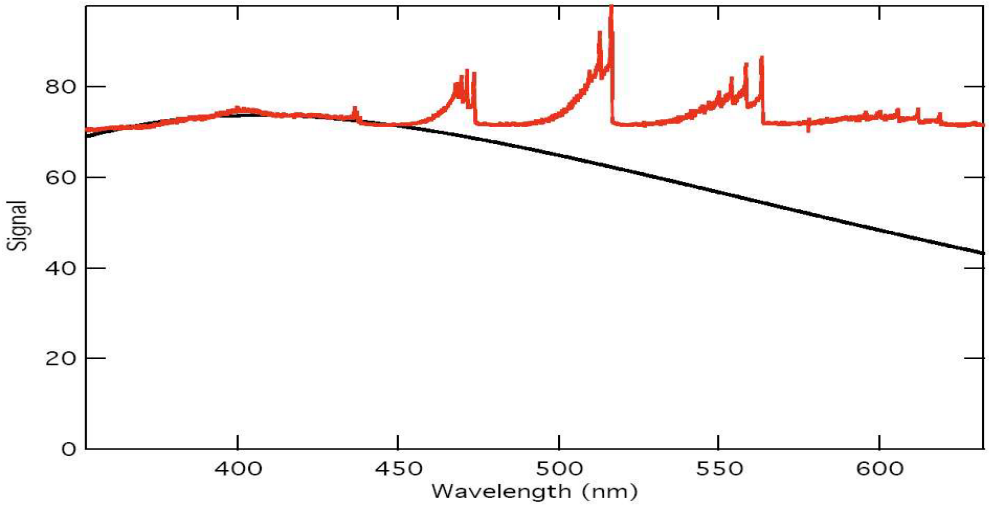

Figure 13. LII fit to the LIB spectrum obtained in 200 torr argon using unfocused laser radiation at 1.1 J cm^{-2} fluence.

As seen in both Figures 12 and 13, the shape of our experimental continuum at 400 nm is sharper than expected for LII, which suggests a molecular origin to the emission instead of incandescence. It was also noted by Rohlfing [18] that the blackbody model cannot reproduce the magnitude and the narrowness of the continuum maximum at 400 nm. Since we have previously indicated that the relatively high pressure rare gas background appears to exclude C_3 emission, we are left to a search for other possible molecules or carbon clusters as sources for the 400 nm continuum.

There are two further sources that we could investigate, either larger linear carbon molecules, C_n with n>3 or large carbon structures, such as polycyclic aromatic hydrocarbons (PAHs) or graphene fragments. According to previous matrix isolation spectroscopic studies [73] linear carbon chains with n>3 have vibronic bands in absorption at wavelengths higher than 400 nm with increasing length of the carbon chain, where only C_3 absorbs or emits. PAH molecules do have emission signatures also near 400 nm [74,75]. However there is no hydrogen in our plasmas, and PAHs could only emerge from water on the surface of our graphite target or from residual water vapor in the LIBS cell. Both of these sources are unlikely, although we have only used rotary backing pump evacuation. In the presence of significant amounts of hydrogen needed for generating PAHs one would expect to see the Balmer beta line near 485 nm [76]. However there is no such emission in our unfocused laser spectra, and only very weak signatures in focused ones. Thus it is not clear how PAHs could arise under our experimental conditions.

As to the absence of the 400 nm continuum under focused laser condition, it is also a possibility

to explain it by considering that while the unfocused laser beam may only have a thermal effect and result in sublimation of C_3 from the target surface, focused irradiation would lead to the ablation of larger clusters. This explanation relies on the assumption that the 400 nm continuum is indeed due to C_3.

An obvious line of possible advance towards the clarification of the source of the 400 nm continuum to solve the C_3 puzzle is to carry out time resolved emission spectroscopy on our plasmas. Such experiments are planned using a time–resolved ICCD camera and a matching grating spectrograph for the range 190–900 nm. This equipment is expected to be used in early 2006 in our laboratory.

Acknowledgment

This work was supported by the Hungarian Basic Research Fundation (OTKA) under contracts T038422 and T046271. We also acknowledge the acquisition of the WaveStar U fiber–optic spectrometer under the OTKA instrument project M036217. C.G.P and J.O.H. acknowledge the partial support received from the UTSI Center for Laser Applications. H.A.M. is supported by the Division of Chemical Sciences, Geosciences, and Biosciences, the Office of Basic Energy Sciences, the U. S. Department of Energy. The authors further acknowledge the help received from Dr. Stephan Irle at the Emory Department of Chemistry and Cherry L. Emerson Center for Scientific Computation University, Atlanta, GA U.S.A. in the theoretical calculations for the $C+C_2 \rightarrow C_3$ reaction.

5 REFERENCES

[1] A. van Orden and R. Saykally, Small carbon clusters: Spectroscopy, Structure and Energetics, *Chem. Rev.* **1998** , *98*, 2313–2356.

[2] W. Huggins, Preliminary Note on the Photographic Spectrum of Comet b 1881, *Proc. Roy.Soc. London* **1881**, *33*, 1–3.

[3] G. Herzberg, Laboratory production of the λ4050 group occurring in cometary spectra; further evidence for the presence of CH_2 molecules in comets, *Astrophys. J.* **1942**, *96*, 314.

[4] A. E. Douglas, Laboratory studies of the λ 4050 group of cometary spectra, *Astrophys. J.* **1951**, *114*, 466–468.

[5] L. Gausset, G. Herzberg, A. Lagerquist and B. Rosen, Spectrum of the C_3 molecule, *Disc. Farad. Soc.* **1963**, *35*, 113–117.

[6] L. Gausset, G. Herzberg, A. Lagerquist and B.Rosen, Analysis of the 4050 Å group of the C_3 molecule, *Astrophys. J.* **1965**, *142*, 45–76.

[7] N. H. Kiess and A. M. Bass, The λ4050 group of cometary spectra in the acetylene–oxygen flame, *J. Chem. Phys.***1954**, *22*, 569–570.

[8] J. G. Phillips and L. Brewer, An ultraviolet continuum in the spectrum of carbon, *Mem. Soc. Roy. Sci. Liege* **1955**, *15*, 341–351.

[9] A. McKellar and E. H. Richardson, Relative spectral gradients of several cool carbon stars in the blue and violet regions, *Mem. Soc. Roy. Sci. Liege* **1955**, *15*, 256–275.

[10] N. H. Kiess and H. P. Broida, Spectrum of the C_3 molecule between 3600 Å and 4200 Å, *Can. J. Phys.* **1956**, *34*, 1471–1479.

[11] J. G. Phillips, Relative temperature coefficients of features in the C_3 spectrum, *Mem. Soc. Roy. Sci. Liege* **1957**, *18*, 538–543.

[12] G. V. Marr, The luminous mantle of fuel–rich oxyacetylene flames, II. Free radical and continuum intensities and their influence on C_3 emissions, *Can. J. Phys.* **1957**, *35*, 1275–1283.

[13] L. Brewer and J. L. Engelke, Spectrum of C_3, *J. Chem. Phys.* **1962**, *36*, 992–998.

[14] H. Henning, Die kontinuierliche Strahlung thermischer Kohlenstoffplasmen, *Z. Astrophys.* **1965**, *62*, 109–120.

[15] D. M. Cooper and J. J. Jones, An experimental determination of the cross section of the Swings band system of

C_3, *J. Quant. Spectrosc. Radiat. Transfer* **1979**, *22*, 201–208.
[16] W. L. Snow and W. L. Wells, The spectral opacity of triatomic carbon measured in a graphite tube furnace over the 280 to 600 nm wavelength range, *J. Chem. Phys.* **1980**, *73*, 2547–2551.
[17] M. Anselment, R. Seth Smith, E. Daykin and L. F. Dimauro, Optical emission studies on graphite in a laser vaporization supersonic jet cluster source, *Chem. Phys. Lett.* **1987**, *134*, 444–449.
[18] E. A. Rohlfing, Optical emission studies of atomic, molecular, and particulate carbon produced from a laser vaporization cluster source, *J. Chem. Phys.* **1988**, *89*, 6103–6112.
[19] P. Monchicourt, Onset of carbon cluster formation inferred from light emission in a laser–induced expansion, *Phys. Rev. Lett.* **1991**, *66*, 1430–1433.
[20] J. Luque, W. Juchmann,and J. B. Jeffries, Spatial density distributions of C_2, C_3 and CH radicals by laser–induced fluorescence in a diamond depositing dc–arcjet, *J. Appl. Phys.* **1997**, *82*, 2072–2081.
[21] G. A. Raiche and J. B. Jeffries, Observation and spatial distribution of C_3 in a DC arcjet plasma during diamond deposition using laser–induced fluorescence, *Appl. Phys.* **1997**, *B64*, 593–597.
[22] N. V. Tarasenko, Laser–induced fluorescence and time–resolved emission spectroscopy of laser ablation plasma, *25th EPS Conf. on Contr. Fusion and Plasma Physics*, *Praha*, 29 June–3 July. ECA **1998**. *22C*, 1647–1650.
[23] S. Arepalli, P. Nikolaev, W. Holmes and C. D. Scott, Diagnostics of laser–produced plume under carbon nanotube growth conditions, *Appl. Phys.* **1999**, *A69*, 1–9.
[24] S. Arepalli, C. D. Scott, Spectral measurements in production of single–wall carbon nanotubes by laser ablation, *Chem. Phys. Lett.* **1999**, *302*, 139–145.
[25] K. Takizawa, K. Sasaki and K. Kadota, Characteristics of C_3 radicals in high–density C_4F_8 plasmas studied by laser–induced fluorescence spectroscopy, *J. Appl. Phys.* **2000**, *88*, 6201–6208.
[26] K. Sasaki, T. Wakasaki and K. Kadota, Observation of continuum optical emission from laser–ablation carbon plumes, *Appl. Surf. Sci.* **2002**, *197–198*, 197–201.
[27] C. Nicolas, J. Shu, D.S. Peterka, M. Hochlaf, L. Poisson, S.R. Leone, M. Ahmed, Vacuum ultraviolet photoionization of C_3, *J. Am. Chem. Soc.* **2005**, *128*, 220–226.
[28] P. S. Skell, J. J. Havel and M. J. McGlinchey, Chemistry and the carbon arc, *Acc. Chem. Res.* **1972**, *6*, 97–105.
[29] H. R. Leider, O. H. Krikorian and D. A. Young, Thermodynamic properties of carbon up to the critical point, *Carbon* **1973**, *11*, 555–563.
[30] C. MacKay, Some primary reactions of free carbon atoms and related chemistry of C_2, C_3 and C_2O, in *Carbenes* (eds.: R. A. Moss and M. Jones, Jr.), Vol. II, J.Wiley and Sons, New York, **1975**, pp. 1–43.
[31] D. M. Mann, A possible first step in carbon particle formation: C_2+C_3, *J. Appl. Phys.* **1978**, *49*, 3485–3489.
[32] J. R. Heath, Q. Zhang, S. C. O'Brien, R. F. Curl, H. W. Kroto, R.E. Smalley, The formation of long carbon chain molecules during laser vaporization of graphite, *J. Am. Chem. Soc.* **1987**, *109*, 359–363.
[33] H. W. Kroto, J. R. Heath, S. C. O'Brien, R. F. Curl, R. E. Smalley, Long carbon chain molecules in circumstellar shells, *Astrophys. J.* **1987**, *314*, 352–355.
[34] J. M. L. Martin, J. P. Francois, and R. Gijbels, On the heat of formation of C_5 and higher carbon clusters, *J. Chem. Phys.* **1991**, *95*, 9420–9421.
[35] M. Martin, C_2 spectroscopy and kinetics, Invited Review, *J. Photochem. Photobiol, A. Chem.* **1992**, *60*, 263–289.
[36] X. Song, Y. Bao, R. S. Urdahl, J. N. Gosine, and W. M. Jackson, Laser–induced fluorescence studies of C_3 formation and isomerization in the 193 nm photolysis of allene and propyne, *Chem. Phys. Lett.* **1994**, *217*, 216–221.
[37] K. A. Gingerich, H. C. Finkbeiner, and R. W. Schmude, Jr., Enthalpies of formation of small linear carbon clusters, *J. Am. Chem. Soc.* **1994**, *116*, 3884–3888.
[38] D. J. Krajnovich, Laser sputtering of highly oriented pyrolytic graphite at 249 nm, *J. Chem. Phys.* **1995**, *102*, 726–743.
[39] T. Kruse and P. Roth, Kinetics of C_2 reactions during high–temperature pyrolysis of acetylene, *J. Phys. Chem.* **1997**, *101*, 2138–2146.
[40] V. S. Burakov, A. F. Bokhonov, M. I. Nedel'ko, N. A. Savastenko and N. V. Tarasenko, Dynamics of the emission of light by C_2 and C_3 molecules in a laser plasma produced by two–pulse irradiation of the target, *J. Appl. Spec.* **2002**, *69*, 907–912.
[41] K. Sasaki, T. Wakasaki, S. Matsui, and K. Kadota, Distributions of C_2 and C_3 radical densities in laser–ablation carbon plumes measured by laser–induced fluorescence imaging spectroscopy, *J. Appl. Phys.* **2002**, *91*, 4033–

4039.
[42] G. Herzberg, K.F. Herzfeld, and E. Teller, The heat of sublimation of graphite, *J. Phys. Chem.* **1937**, *41*, 325–331.
[43] E. Wigner and E. E. Witmer, On the structure of the spectra of two–atomic molecules according to quantum mechanics, *Z. Phys.* **1928**, *51*, 859.
[44] G. Herzberg, Molecular Spectra and Molecular Structure, III. Electronic spectra and Electronic Structure of Polyatomic Molecules, Van Nostrand, New York, 1966, pp. 284.
[45] K. E. Shuler, Adiabatic correlation rules for reactions involving polyatomic intermediate complexes and their application to the formation of OH ($^2\Sigma^+$) in the H_2 –O_2 flame, *J. Chem. Phys*, **1953**, *21*, 624–632.
[46] G. Monninger, M. Förderer, P. Gürtler, S. Kalhofer, S. Petersen, L. Nemes, P. G. Szalay, and W. Krätschmer, Vacuum ultraviolet spectroscopy of the carbon molecule C_3 in matrix isolated state: Experiment and theory, *J. Phys. Chem. A* **2002**, *106*, 5779–5788.
[47] I. Cermak, M. Förderer, S. Kalhofer, H. Stopka–Ebeler, and W. Krätschmer, Laser–induced emission spectroscopy of matrix–isolated carbon molecules: experimental setup and new results on C_3, *J. Chem. Phys.* **1998**, *108*, 10129–10142.
[48] H. Choi, R. T. Bise, A. A. Hoops, D. H. Mordaunt, and D. M. Neumark, Photodissociation of linear carbon clusters C_n (n= 4–6), *J. Phys. Chem. A* **2000**, *104*, 2025–2032.
[49] M. E. Geusic, T. J. McIlrath, M. F. Jarrold, L. A. Bloomfield, and R. R. Freeman, Photofragmentation of mass–resolved carbon cluster ions: observation of a 'magic' neutral fragment, *J. Chem. Phys.* **1986**, *84*, 2421–2422.
[50] Z. Cao, M. Mühlhäuser, M. Hanrath and S. D. Peyerimhoff, Study of possible photodissociation channels in linear carbon clusters C_n (n=4–6), *Chem. Phys. Lett.* **2002**, *351*, 327–334.
[51] H. Fueno and Y. Taniguchi, Ab initio molecular orbital study of the isomerization reaction surfaces of C_3 and C_3^-, *Chem. Phys. Lett.* **1999**, *312*, 65–70.
[52] P. Zhang, Q. Wang, S. Irle, and K. Morokuma, Ab initio MRCISD study of the $^1C_2 + C(^3P) \rightarrow {}^{1,3} C_3$ reaction, to be published.
[53] F. Varga and L. Nemes, Emission spectroscopic studies of laser–induced graphite plasmas, J. *Mol. Struct.* **1999**, *480–481*, 273–279.
[54] C. G. Parigger, J. O. Hornkohl, A. M. Keszler, and L. Nemes, Laser–induced breakdown spectroscopy: molecular spectra with BESP and NEQAIR, Laser Induced Plasma Spectroscopy and Applications, *OSA Technical Digest Series*, *Opt. Soc. Amer.* **2002**, *81*, 102–103.
[55] C. G. Parigger, J. O. Hornkohl, A. M. Keszler, and L. Nemes, Measurement and analysis of atomic and diatomic carbon spectra from laser ablation of graphite, *Appl. Opt.* **2003**, *42*, 6192–6197.
[56] A. Keszler and L. Nemes, Time averaged emission spectra of Nd:YAG laser induced carbon plasmas, *J. Mol. Struct.* **2004**, *695–696*, 211–218.
[57] L. Nemes, A.M. Keszler, J.O. Hornkohl, and C. G. Parigger, Laser–induced carbon plasma emission spectroscopic measurements on solid targets and in gas–phase optical breakdown, *Appl. Opt.* **2005**, *44*, 3661–3667.
[58] J. O. Hornkohl, C. G. Parigger, and L. Nemes, A new diatomic Hönl–London factor computer program, *Appl. Opt.* **2005**, *44*, 3686–3695.
[59] A.P. Thorne, U. Litzen, and S. Johansson, *Spectrophysics: Principles and Applications*, Springer Verlag, Berlin, 1999.
[60] http://www.chemistry.ohio–state.edu/~vstakhur/C3bands.php.
[61] Ch. Jungen and A. J. Merer, Orbital angular momentum in triatomic molecules. IV. The $A^1\Pi_u$ state of C_3, *Mol. Phys.* **1980**, *40*, 95–114.
[62] E. A. Rohlfing, Laser–induced–fluorescence spectroscopy of jet–cooled C_3, *J. Chem. Phys.* **1989**, *91*, 4531–4542.
[63] E. A. Rohlfing and J. E. M. Goldsmith, Stimulated–emission pumping spectroscopy of jet–cooled C_3: antisymmetric stretch–bend levels, *J. Opt. Soc. Amer.* **1990**, *A7*, 1915–1923.
[64] J. Baker, S. K. Bramble, and P. A. Hamilton, A hot band LIF study of the $A^1\Pi_u - X^1\Sigma^+_g$ transition in C_3, *Chem.Phys. Lett.* **1993**, *213*, 297–302.
[65] W. J. Balfour, J. Cao, C. V. V. Prasad, and C. X. W. Quian, Laser–induced fluorescence spectroscopy of the$A^1\Pi_u - X^1\Sigma^+_g$ transition, *J. Chem. Phys.* **1994**, *101*, 10343–10349.
[66] M. Izuha and K. Yamanouchi, New vibronic bands of the laser–vaporized C_3 cluster. Determination of the ν_3 fundamental in the $A^1\Pi_u$ state, *Chem. Phys. Lett.* **1995**, *242*, 435–442.
[67] M. Izuha and K. Yamanouchi, New A–X vibronic bands of laser–vaporized C_3, *J. Chem. Phys.* **1998**, *109*, 1810–

1817.

[68] B. J. McCall, R. N. Casaes, M. Ádámkovics, and R. J. Saykally, A re–examination of the 4051 Å band of C_3 using cavity ringdown spectroscopy of a supersonic plasma, *Chem*. *Phys*. *Lett*. **2003**, *374*, 583–586.

[69] J. O. Hornkohl, C. Parigger and J. W. L. Lewis, Temperature measurements from CN spectra in a laser–induced plasma *J*. *Quant*. *Spectr*. *Rad*. *Transf*. **1991**, *46*, 405–411.

[70] C. G. Parigger, D. H. Plemmons, J. O. Hornkohl, and J. W. L. Lewis, Spectroscopic temperature measurements in a decaying laser–induced plasma using the C_2 Swan system, *J. Quant*. *Spectrosc*. *Radiat*. *Transfer* **1994**, *52*, 707–711.

[71] T. Wakasaki, K. Sasaki, and K. Kadota, Collisional quenching of C_2($d^3\Pi_g$) and $C_3(A^1\Pi_u)$ and its application to the estimation of absolute particle density in laser–ablation carbon plumes, *Jpn*. *J*. *Appl*. *Phys*. **2002**, *41*, 5792–5796.

[72] H. A. Michelsen, Understanding and predicting the temporal response of laser–induced incandescence from carbonaceous particles, *J. Chem*. *Phys*. **2003**, *118*, 7012–7045.

[73] S. Kalhofer, I. Cermak, M. Förderer, G. Monninger, I. Cermaková, W. Krätschmer, P. Gürtler, and S. Petersen, Emission and absorption spectroscopy of matrix isolated carbon molecules, *EUCMOS XXIV*, Prague, Czech Republic, 23–28 August, **1998**.

[74] F. Ossler, T. Metz, and M. Aldén, Picosecond laser–induced fluorescence from gas–phase polycyclic aromatic hydrocarbons at elevated temperatures, I. Cell measurements, *Appl*. *Phys B* **2001**, *72*, 465–478.

[75] F. Ossler, T. Metz, and M. Aldén, Picosecond laser–induced fluorescence from gas–phase polycyclic aromatic hydrocarbons at elevated temperatures. II. Flame–seeding measurements, *Appl*. *Phys*. *B* **2001**, *72*, 479–489.

[76] C. G. Parigger, D. H. Plemmons, and E. Oks, Balmer series H_β measurements in a laser–induced hydrogen plasma, *Appl*. *Opt*. **2003**, *42*, 5992–6000.

[77] D. C. Tyte, S. H. Innanen, and R. W. Nicholls, *Indentification Atlas of Molecular Spectra*, *Part 5*. *The* C_2 $A^3\Pi_g$ – $X'^3\Pi_u$ *Swan System*, York University, Toronto, 1967.